

DEEP TRANSFORMERS THIRST FOR COMPREHENSIVE-FREQUENCY DATA

Rui Xia, Chao Xue, Boyu Deng, Fang Wang, Jingchao Wang*

Academy of Military Science of the People's Liberation Army, Beijing, China
xiarui414@foxmail.com, {wangjc.2000, xuec11}@tsinghua.org.cn, kdydyb2014@sina.com

ABSTRACT

Current researches indicate that inductive bias (IB) can improve Vision Transformer (ViT) performance. However, they introduce a pyramid structure concurrently to counteract the incremental FLOPs and parameters caused by introducing IB. This structure destroys the unification of computer vision and natural language processing (NLP) and complicates the model. We study an NLP model called LSRA [1], which introduces IB with a pyramid-free structure. We analyze why it outperforms ViT, discovering that introducing IB increases the share of high-frequency data in each layer, giving "attention" to more information. As a result, the heads notice more diverse information, showing better performance. To further explore the potential of transformers, we propose EIT, which Efficiently introduces IB to ViT with a novel decreasing convolutional structure under a pyramid-free structure. EIT achieves competitive performance with the state-of-the-art (SOTA) methods on ImageNet-1K and achieves SOTA performance over the same scale models which have the pyramid-free structure.

Index Terms— Image Classification, Vision Transformer, Wave Filter, Frequency Data, Multi-Heads Diversity

1. INTRODUCTION

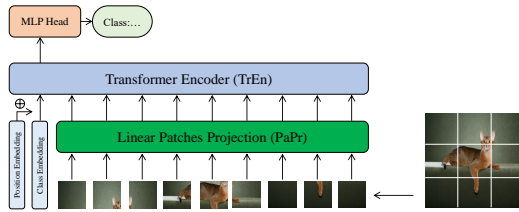


Fig. 1. The brief structure of ViT.

In recent years, Transformer [2] has swept the field of natural language processing (NLP) due to its superior performance. The fields of the computer vision (CV) [3, 4] and even the multi-agent reinforcement learning (MARL) [5, 6] are also gradually infiltrated by this famous technology. Vision Transformer (ViT) [3] is the first CV model which is completely based on the Transformer architecture and achieves better performance on ultra-large-scale image classification task than the convolutional neural networks (CNN). ViT is also the first model trying to break the barrier of unifying the CV and NLP with the same backbone and achieved a breakthrough. Such a model is beneficial for the future research on the MultiModal networks [7]. Specifically, ViT divides images into several non-overlapping patches to correspond the *tokens* in NLP, and uses the full-Transformer architecture to model the patches and complete the image classification task. The brief structure of ViT is shown in Fig. 1.

The original ViT relies on the ultra-large-scale datasets to perform better than the same scale CNN [3]. The strong data augmentation can free ViT from the dependence on the ultra-large-scale datasets [13]. However, many studies have shown that ViT trained with strong data augmentation is still suboptimal [8, 9, 10, 11, 12, 14]. One reason is that Transformers lack some

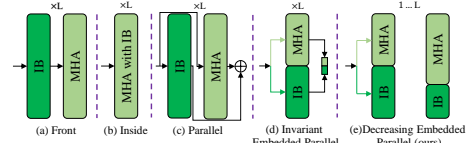


Fig. 2. The ways of introducing IB. (a) Data is pre-processed by IB structure [8, 9, 10]. (b) MHA with built-in IB [11]. (c) MHA handles all data together with the module with IB structure [12]. (d) The MHA and the IB structure each process a invariant portion of the data [1]. (e) IB structure in the previous layer process less data than those in the next layer.

of the properties similar to inductive biases (IB) inherent to CNN, such as locality [3]. Many studies have been explored on introducing the IB into ViT, such as the locality-based methods like TNT [8] and T2T [10], or CNN based methods like EA [12], CvT [11], Swin [9] and ViT_C [14]. In summary, the recent methods of introducing IB can be summarized in three categories, as shown in the first three items of Fig.2. The aforementioned researches have experimentally demonstrated that the introducing IB can improve the performance of ViT. Since the introducing IB brings the redundant structures, a few of them suffer from a significant increase in parameters and FLOPs [8, 10, 12]. To solve this problem, quite a few of them further introduce the pyramid structure [9, 11, 14]. However, the pyramid structure destroys the structure of Transformer and departs from the original intention of ViT, which intends to unify CV and NLP by a same structure. Moreover, the pyramid structure complicates the model, which is not conducive to further optimization.

In this work, to ensure the unification of CV and NLP and keep the model brevity while introducing IB, we study LSRA [1], a model of NLP. Its brief structure is shown in Fig.2-(d), which divides the data stream along the channel dimension to Multi-Head Attention (MHA) and IB, achieving introducing IB without increasing FLOPs and parameters. We analyze why it outperforms ViT finding that the lack of IB in ViT is manifested explicitly by the small diversity of head-attention distances (Head Diversity) in the deep layers, which causes a degradation in the performance. We qualitatively analyze the reasons for the small Head Diversity of ViT's deep layers and explain how the LSRA introduces IB into ViT from the perspective of a filter. As a high-frequency filter, the IB improves the deep layers' share of high-frequency data, giving 'attention' more comprehensive information, thus boosting Head Diversity. However, we find LSRA suffers from the inefficient introducing IB, resulting in small Head Diversity and performance limitations.

Based on this, we propose a model called EIT, which can Efficiently introduce the IB to the ViT under pyramid-free structures and with fewer parameters and FLOPs, as shown in Fig.2-(e). We make the following two changes to get the Decreasing Embedded Parallel Structure (Decreasing Structure): 1) the linear Patches Projection (PaPr) of ViT is replaced by a convolutional layer plus a maximum pooling layer, which is called EIT^P; 2) a decreasing convolutional structure is introduced to the MHA of Transformer Encoder (TrEn), by which the embedding's different channel dimensions are processed, respectively. We validated the performance of EIT on four small-scale datasets and a large-scale dataset showing that the EIT outperforms the similar ViT-like methods (ViTs). Moreover, the proposed Decreasing Structure is generally applicable to Transformer-based architectures and further impacts a broader range of applications. We summarize the contributions as follows:

1. To the best of our knowledge, we first find and explain that introducing

* Corresponding author

Supported by the National Natural Science Foundation of China (Grant No. 62022093 and No. 62101587).

Code: <https://github.com/MrHaiPi/EIT>

IB can increase the share of high-frequency data in each layer, giving "attention" more comprehensive data. Comprehensive data improves the diversity of head-attention distances in Transformers, which causes performance improvement.

- We propose a novel Decreasing Structure based on the principle that MHA and IB are low-pass filters and high-pass filters. Such a structure can efficiently introduce IB to ViT with fewer parameters and FLOPs with a pyramid-free structure, ensuring the unification of CV and NLP.
- We conduct comprehensive experiments that show EIT achieves promising and competitive results than the similar representative state-of-the-art methods currently available. In particular, EIT achieves state-of-the-art performance over the other same scale models which have a pyramid-free structure.

2. RELATED WORKS

2.1. Vision Transformer

Although there were many Transformer-based models in the CV field, ViT [3] was the first model based entirely on Transformer and tried to unify the CV and NLP with the same network structure. In its implementation, ViT first split an image into non-overlapping patches, then mapped the patches into patches embedding by a linear mapping layer. Finally, it classified the images by connecting multiple standard TrEn. However, the ViT, which is trained with ultra-large-scale datasets (e.g., ImageNet-21k and JFT-300M) [3] and strong data augmentation (e.g., MixUp [15], CutMix [16] and Erasing [17]), is still suboptimal, with the reason of IB lacking [8, 9, 10, 11, 12, 14]. In this paper, we study how to efficiently introduce IB to ViT.

2.2. Introduce Inductive Biases to ViT

Many methods have been proposed to introduce IB to ViT. For example, Transformer-in-Transformer (TNT) [8] introduced the Transformer module inside patches to model a more detailed pixel-level representation. Tokens-to-Token (T2T) [10] stitched together neighbouring embedding to form a new embedding in the original location to change ViT's PaPr. Such an operation could preemptively improve the similarity of neighbouring, which in turn introduced IB. CvT [11] introduced IB to both PaPr and TrEn by convolution operation with a hierarchical structure. Specifically, CvT changed the original linear mapping of ViT to a convolutional mapping in both PaPr and TrEn. The stride of convolution was smaller than the kernel size. ViT_C [14] changed the PaPr with Convolutional Stem to help transformers see better. Besides, in NLP, Long-Short Range Attention (LSRA) [1] introduced Lite Transformer Block (LTB) to TrEn, which divided half of the data to be processed by MHA along the channel dimension to the convolutional layer. Summarizing the above works, we can find two phases to introduce the IB to ViT. One is the PaPr phase, and the other is the TrEn phase. Table 1 summarizes the contributions of the above works.

Table 1. Representative works of introducing IB.

Method	Position Encoding	Introduce IB to PaPr phase	Introduce IB to TrEn phase	Pyramid
LSRA [1]	Cosine	None	Lite Transformer Block (LTB)	×
ViT [3]	Trainable	None	None	×
T2T [10]	Trainable	Concatenate	None	×
TNT [8]	Trainable	Patch + Pixel	Patch + Pixel	×
CvT [11]	None	Convolutional Embedding (CvT ^P)	Convolutional Mapping QKV (CvT ^T)	✓
ViT _C [14]	Trainable	Convolutional Stem (CoSt)	None	✓
EIT(ours)	None	Convolutional Embedding and Maxpool (EIT ^P)	Decreasing Convolution (EIT ^T)	×

However, the above works suffer from the inefficient introducing IB or the inability to reconcile the contradiction between pyramid-free structures and fewer FLOPs/parameters. In contrast to these concurrent works, our method ensures both the efficiency of IB introduction and the pyramid-free structures without increasing the FLOPs/parameters.

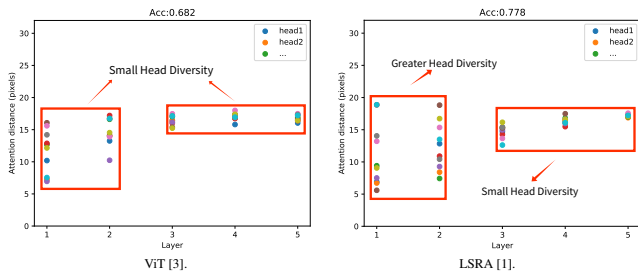


Fig. 3. The distribution of the head-attention distances for each layer. The models consist of five TrEns, and each TrEn contains ten heads. The above results are from training and testing on the Cifar10 [18]. Attention distance is computed for 2000 example images from Cifar10 by summing the distance between the selected query pixel and all other pixels, weighted by the attention weight [3]. The variance of the attention distances at each layer approximates the Head Diversity. The figure shows that the Head Diversity of layers 3, 4, and 5 of LSRA is basically the same as ViT. The LSRA's Head Diversity of the first two layers are larger than ViT, thus performs better.

3. OUR APPROACH

3.1. Motivation

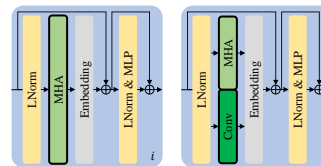


Fig. 4. The main structure of ViT (left) and LSRA (right).

We determine that LSRA [1], a model of NLP as shown in Fig.4 (right), can also perform better than ViT [3] for image classification. When we investigated the performance improvement of LSRA, we found that the reason for the poor performance of ViT is that it has small Head Diversity, as shown in Fig.3. The reason why LSRA outperforms than ViT is that the introducing IB improves the Head Diversity and thus enables Transformers to have more comprehensive information. However, as we can see, the Head Diversity of LSRA's deep layers is still small, so we believe that the introducing IB of LSRA is not efficient enough. We speculate that the network's performance will be further improved if IB is introduced more efficiently to make the Head Diversity at the deep layers greater. To further improve the efficiency of introducing IB, we investigate why LSRA brings more IB to the network than ViT and why LSRA cannot bring IB to the leaning back layers. Since the main structure of LSRA is the Invariant Embedded Parallel Structure (Invariant Structure), we first investigate it.

3.2. Why Does It Work?

In comparison with ViT, LSRA adds a convolution module in parallel at the MHA, as shown in Fig.4. The Convs (i.e., IB Structure) and MHAs each process half of the data along the channel dimension. Since its structure is invariable, all the layers repeat the same operation.

Since the MHAs are the low-pass filters, they reduce the high-frequency data (HFD) share layer by layer [19]. Because the HFD share drops with each layer, the deep MHAs have difficulty detecting the HFD, i.e., the short-distance information. As a result, the attention distances of ViT converge to a greater value as the layers deepen. The fact that the deep layers do not adequately utilize the HFD, is the reason of ViT's poor performance.

In comparison with ViT, LSRA introduces the convolutions, the high-pass filters [19], to improve the HFD share. As a result, LSRA's HFD share drops more slowly, which makes it more use of the HFD, resulting in slower convergence of attention distance. Also, the improved HFD utilization leads to improved performance.

3.3. Why Is It Suboptimal?

You may now ask: why in a structure like Embedded Parallel, where MHAs and Convs each process half of the data along the channel dimension, does it still cause a drop in HFD share? We are confident that it is because the Receptive Field of Convs become larger as the layers increase [20].

We know that HFD corresponds to local information, which requires a small Receptive Field. When the Receptive Field of Conv increases, its high-pass filtering ability decreases. For the network, it means inefficient introduction of IB. In contrast, MHA is a global attention receptor, and its Receptive Field is the whole feature map. The receptive field of MHA does not change as the layers increase, i.e., its low-pass filtering ability does not become weaker as the layers increase. Since the high-pass filtering ability of Conv gradually becomes weaker and the low-pass filtering ability of MHA remains the same, the overall HFD share decreases as a result.

3.4. How to Do?

To increase the HFD share of the deeper layers, an intuitive idea is to increase the share of data processed by the deeper Convs, called Increasing Structure. In the Increasing Structure, the deep MHAs share is decreasing, and the Convs share is increasing. The decrease of deep MHAs share reduces low-frequency data (LFD), and the increase of deep Convs share does not increase HFD (we will discuss this issue later). As a result, this structure increases the HFD share of the data by reducing LFD. However, our ultimate goal is to give MHAs more comprehensive information, so we cannot increase the HFD share by reducing LFD.

Why the increase of deep Convs share does not increase HFD? Because the HFD has been filtered out by the shallow layers. We can not use a low-pass filter to filter out the high-frequency components of the data and then use a high-pass filter to extract its high-frequency components. This is impossible because the high-frequency components have already been removed, and you cannot get the components that the high-pass filter has removed, as shown in Fig.5.

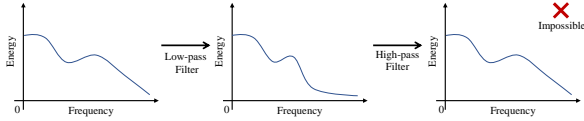


Fig. 5. Low/High-Pass Filter Processes Data.

We think a reasonable approach is to increase the proportion of Conv processed data in the shallow layers and keep as much HFD as possible for the deep layers. At the same time, decreasing the proportion of MHA processed data in the shallow layers to reduce the weakening ability of MHA on HFD. As a result, making more HFD can be passed to the deeper layers of the network. Of course, we cannot just increase the HFD share in the network because our goal is to give MHA more comprehensive information rather than just HFD. For this reason, we also increase the proportion of data processed by the MHA in the deeper layers.

3.5. Network Architecture

3.5.1. EIT

Based on the above analysis, we design a Decreasing Structure to improve the efficiency of the IB introduction. The architecture of the proposed model is shown in Fig.6. We propose two simple structures called EIT^P (EIT for PaPr) and EIT^T (EIT for TrEn) to form a complete Decreasing Structure.

3.5.2. EIT for PaPr

EIT^P uses a convolution layer with a stride smaller than the kernel size, i.e., there are overlapping patches, which can improve the locality, result in introducing IB efficiency of PaPr. However, it also means we will introduce redundant patches to the TrEns, introducing excess FLOPs. To solve this problem without seriously destroying the similarity of the adjacent patches, we filter out the redundant patches by a maximum pooling layer.

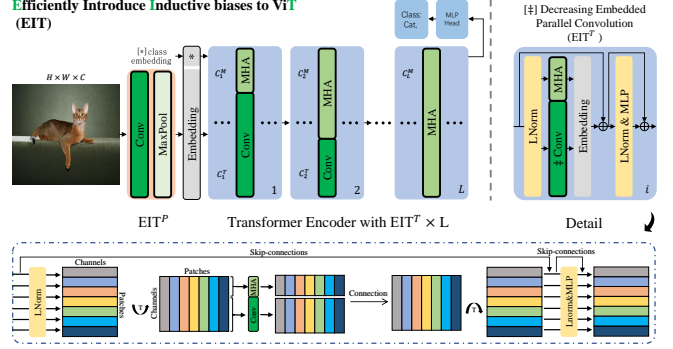


Fig. 6. Model Overview. The backbone of EIT is the same as ViT. EIT^T and MHA each process all the patches embedding in **different channel dimensions**. C_i^T and C_i^M are the number of channels processed by EIT^T and MHA, respectively.

3.5.3. EIT for TrEn

The structure of introducing IB in LSRA [1] contains one activation layer, one convolutional layer, and one fully connected layer. EIT^T contains only one layer of convolution. Because we believe that if we aim to use the property of the high-pass filter of the convolution, we only need to have one convolutional layer. Multiple convolutional layers increase the Receptive Field and weaken the EIT^T 's high-pass filter ability. Other types of layers (e.g., activation layers, fully connected layers) do not enhance EIT^T 's high-pass filtering ability, and we consider them dispensable.

4. EXPERIMENTS

4.1. Set up

We use four popular small-scale datasets and one large-scale dataset to evaluate the performance of EIT: Cifar10/100 [18], Fashion-Mnist [21], Tiny ImageNet-200 [22], and ImageNet-1K [20]. The model configuration is detailed in Table 2 and the training configuration is in Table 4 and Table 3, respectively. We train our model on ImageNet-1K with strong data augmentation. Specifically, we adopt the same data augmentations (RandAugment [23], MixUp [15], CutMix [16] and Erasing [17]) as DeiT [13].

Table 2. Details of EIT model variants. EIT16/4/3 indicates that the convolutional kernel size used in EIT^P is 16, the stride of EIT^P is 4, and the kernel size and stride of the maxpool in EIT^P is 3, and C is the number of channels (i.e., embedding dimension). The kernel size and stride of EIT^T are 3 and 1, respectively, by default. The "Params" is for a 1000-category classification task with an input image size of 224×224 . We utilize standard convolutions in EIT^P and depth-wise separable convolution [24] in EIT^T .

Model	C	EIT^P	EIT^T	Layers	MLP Size	Heads	Params.
EIT16/4/3-Mini	250			5		10	3.5M
EIT16/4/3-Tiny	330	$C@Conv:(16,16,4)$	$C^T@$	8	$4C$	10	8.9M
EIT16/4/3-Base	400	Maxpool:(3,3,3)	Conv:(3,3,1,groups= C^T)	10		16	16.0M
EIT16/4/3-Large	464			12		16	25.3M

Table 3. Details of model training on the small-scale datasets. All the models are trained with a total batch size of 25 for 300 epochs.

Optimizer	Aug.	Scheduler	LR	LR min	Drop	Att. Drop	DropPath
SGD	H. flip	Cosine	1e-3	1e-5	0.2	0.15	0.2

4.2. Comparison on the ImageNet-1K

Table 5 and Fig.7 discuss EIT's performance on the ImageNet-1K with other state-of-the-art methods.

When compared to MobileNetV1 [24], EIT16/4/3-Mini obtains 70% Top-1 accuracy with 83% parameters in models with pyramid structure. In

Table 4. Details of model training on the ImageNet-1K. We train our models on $4 \times V100-32G$ with a total batch size of 1024, 1024, 512 and 512 for EIT-Mini, EIT-Tiny, EIT-Base and EIT-Large, respectively, for 300 epochs.

Optimizer	LR	LR decay	LR min	Weight decay	Warmup epochs	Label smoothing	Dropout	Stoch. Depth	Repeated Aug	H. flip	RRC	Rand Augment	Mixup alpha	Curmix alpha	Erasing prob.	Test crop ratio	Loss
AdamW	1e-3	cosine	1e-5	0.05	5	0.1	0	0	0	✓	✓	9/0.5	0.8	1.0	0.25	0.875	CE

comparison to ResNet152 [25], EIT16/4/3-Tiny achieves 78% Top-1 accuracy with 15% parameters and 35% FLOPs. EIT16/4/3-Base obtains 80.6% Top-1 accuracy, which is 0.7% higher than RegNetY-8G [26], with 41% parameters and 82% FLOPs. EIT16/4/3-Mini obtains 0.4% higher Top-1 accuracy with 61% parameters than HVT-Ti-1 [27]. EIT16/4/3-Tiny provides a similar Top-1 accuracy with 68% parameters as PVTv2-B1 [28]. EIT16/4/3-Base obtains the similar Top-1 accuracy, with 80% and 55% parameters, respectively, as CvT-13 [11] and Swin-T [9]. EIT16/4/3-Large provides a similar Top-1 accuracy with 78% and 80% parameters, respectively, as CvT-21 [11] and Next-ViT-S [29].

In models with a pyramid-free structure, EIT16/4/3-Base obtains a similar Top-1 accuracy as T2T-14 [10] while reducing 27% parameters. When compared to the TNT-S [8], the EIT16/4/3-Base achieves the similar Top-1 accuracy with 67% parameters. EIT16/4/3-Tiny achieves 3.2% higher Top-1 accuracy with 7% FLOPs and 10% parameters than ViTB/16 [3]. Furthermore, compared to DeiT-B [13], EIT16/4/3-Large achieves the same Top-1 accuracy with 29% parameters and 59% FLOPs.

EIT achieves promising and competitive results than the similar representative state-of-the-art methods currently available. In particular, EIT achieves state-of-the-art performance over the other same scale models which have a pyramid-free structure. The models with pyramid structure generally contain fewer FLOPs and parameters than the models with pyramid-free structure. In terms of FLOPs, EIT closes the 'gap' between pyramid-free and pyramid structures and delivers better results in terms of parameters. This signifies that the pyramid structure is not required for image processing. The pyramid-free structures also keep the model brevity, facilitating the adjustment of model parameters.

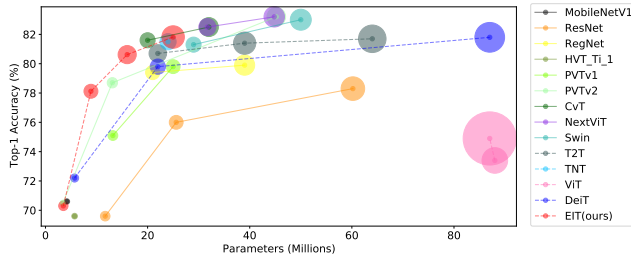


Fig. 7. Comparison on the ImageNet-1K. The size of the circle corresponds to FLOPs. The solid line and dashed line represent the model with pyramid structure and the model with pyramid-free structure, respectively. Existing networks with a pyramidal structure are generally better than networks with a pyramid-free structure. Our EIT beats the pyramid structure with a pyramid-free structure. Because of the efficient use of comprehensive-frequency data by EIT, the parameter utilization of EIT is the highest.

4.3. Comparison on the small-scale datasets

In this section we discuss the performance of CvT [11], LSRA [1], ViT_C [14] and EIT in terms of IB introduction for the same architecture based on small-scale datasets. In the following experiments, we use Model Idx to denote the model.

We discuss the performance of EIT based on EIT3/1/4-Mini. We compare how EIT introduces IB in both phases (PaPr and TrEn) of ViT with that of CvT [11], LSRA [1] and ViT_C [14], with the same network architecture.

Table 5. Comparison on the ImageNet-1K. The image size is 224×224 .

Model	Source	Pyramid	FLOPs	Param	Top-1
MobileNetV1 [24]	arXiv2017	✓	0.58G	4.2M	0.706
ResNet18 [25]	CVPR2016	✓	1.82G	11.7M	0.696
ResNet50 [25]	CVPR2016	✓	3.77G	25.6M	0.760
ResNet152 [25]	CVPR2016	✓	11G	60.2M	0.783
RegNetY-4G [26]	CVPR2020	✓	4G	21M	0.794
RegNetY-8G [26]	CVPR2020	✓	8G	39M	0.799
HVT-Ti-1 [27]	ICCV2021	✓	0.64G	5.7M	0.696
PVTv1-Tiny [30]	ICCV2021	✓	1.90G	13.2M	0.751
PVTv1-Small [30]	ICCV2021	✓	3.80G	25M	0.798
PVTv2-B0 [28]	CVM2022	✓	0.6G	3.4M	0.705
PVTv2-B1 [28]	CVM2022	✓	2.1G	13.1M	0.787
PVTv2-B3 [28]	CVM2022	✓	6.9G	45.2M	0.832
CvT-13 [11]	ICCV2021	✓	4.5G	20M	0.816
CvT-21 [11]	ICCV2021	✓	7.1G	32M	0.825
Swin-T [9]	ICCV2021	✓	4.5G	29M	0.813
Swin-S [9]	ICCV2021	✓	8.7G	50M	0.830
Next-ViT-S [29]	ECCV2022	✓	5.8G	31.7M	0.825
Next-ViT-B [29]	ECCV2022	✓	8.3G	44.8M	0.832
T2T-14 [10]	ICCV2021	×	6.1G	22M	0.807
T2T-19 [10]	ICCV2021	×	9.8G	39M	0.814
T2T-24 [10]	ICCV2021	×	15G	64M	0.817
TNT-S [8]	NIPS2021	×	5.2G	24M	0.815
ViTB/32 [3]	ICLR2021	×	13G	88M	0.734
ViTB/16 [3]	ICLR2021	×	56G	87M	0.749
DeiT-T [13]	ICML2021	×	1.3G	5.7M	0.722
DeiT-S [13]	ICML2021	×	4.6G	22M	0.798
DeiT-B [13]	ICML2021	×	17.5G	87M	0.818
EIT16/4/3-Mini	-	×	1.73G	3.5M	0.700
EIT16/4/3-Tiny	-	×	3.84G	8.9M	0.781
EIT16/4/3-Base	-	×	6.52G	16.0M	0.806
EIT16/4/3-Large	-	×	10.0G	25.3M	0.818

The results are shown in Table 6, showing that both structures of EIT exhibit more efficient introducing IB. On the four datasets, compared with ViT, EIT has the average improvement of 12.6% with fewer parameters and FLOPs. Compared with CvT, LSRA and ViT_C, the average improvement of EIT are 6.4%, 7.3% and 10.7%, respectively.

Table 6. Comparison with the ViTs. The structural parameters (C, Layers, MLP size and Heads) of ViTs are the same. All the convolution of ViTs in PaPr is standard convolution. * We did not use the pyramid structure of the models to ensure the fairness of the comparison of ViTs. The convolutional kernel size of CvT^P is 4, and the stride is 2. The value of n in ViT_C is 2, the convolutional kernel size is 4, and the stride is 2.

Model Idx	Method (ViTs)	Intro. IB to PaPr Phase	Intro. IB to TrEn Phase	FLOPs	Param.	Cifar10	Cifar100	Fashion Mnist	Tiny ImageNet	Avg.
1.1	ViT [3]	None	None	0.515G	3.798M	0.682	0.413	0.888	0.246	0.557(+0.0%)
1.2	LSRA [1]	None	LTB	0.390G	2.924M	0.778	0.477	0.910	0.276	0.610(+5.3%)
1.3	CvT* [11]	CvT ^P	None	2.296G	3.846M	0.738	0.452	0.899	0.280	0.592(+3.5%)
1.4		None	CvT ^T	0.763G	5.706M	0.712	0.414	0.909	0.233	0.567(+1.0%)
1.5		CvT ^P	CvT ^T	3.277G	5.755M	0.777	0.497	0.914	0.288	0.619(+6.2%)
1.6	ViT _C * [14]	CoSt	None	0.553G	4.108M	0.700	0.431	0.902	0.269	0.576(+1.9%)
1.7	EIT3/1/4-Mini	EIT ^P	None	0.527G	3.793M	0.746	0.479	0.911	0.283	0.605(+4.8%)
1.8		None	EIT ^T	0.501G	3.771M	0.818	0.523	0.922	0.313	0.644(+8.7%)
1.9		EIT ^P	EIT ^T	0.428G	3.095M	0.855	0.605	0.926	0.346	0.683(+12.6%)

4.4. Visualization

To verify if the performance improvement of EIT is due to the improvement of Header Diversity of deep MHAs, we computed the attention distances of ViT, LSRA, and EIT, with the Model Idx 1.1, 1.2, and 1.9 respectively, as shown in Fig.9. The attention distances are obtained by the same operation mentioned in Fig.3.

We speculate in Section 3.2 that the poor performance of small Head Diversity is due to the smaller Header Diversity representing less HFD share in received data. To verify this speculation, we calculate the frequency share distribution of each layer's input by summing each channel's two-dimensional Fourier Transform for 2000 images of Cifar10 [18]. For the i -layer's input $x_i \in \mathbb{R}^{(1+H_i W_i) \times C_i}$, the j -frequency share γ_{ij} is defined

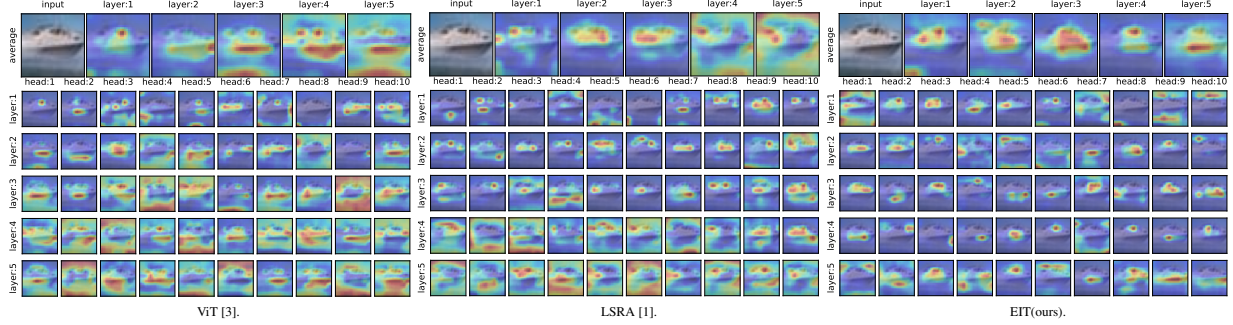


Fig. 8. Attention Maps of ViTs. ViT’s MHA attention range is expanding layer by layer. LSRA’s attention range expands more slowly than ViT due to its improvement of HFD. Since the EIT guarantees the deep MHA’s HFD, the attention can still focus on short-distance. This means the deep MHAs are not actively paying attention to the low frequencies (long-distance). The real reason is that they receive too little HFD compared with LFD. That is why the attention potential of ViT is not being fully exploited, resulting in poor performance.

as follows.

$$\gamma_{ij} = \frac{\sum_c |F_j(\text{Reshape}2D(x_i[1:c]))|}{\sum_f \sum_c |F_f(\text{Reshape}2D(x_i[1:c]))|} \quad (1)$$

where $F(\cdot)$ is the two dimensional Fourier Transform, and $F_j(\cdot)$ represents the component with frequency j . c and f are the channel index and frequency index, respectively. The results are as shown in Fig.10.

To visualize the effect of HFD on the MHA of each layer, we calculate the attention maps by randomly selecting one image from Cifar10, as shown in Fig.8. The attention maps of each layer are obtained by averaging that of heads. The attention maps of each head are the average of all channels.

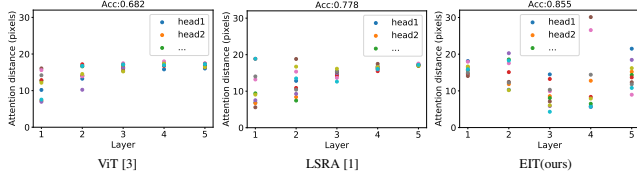


Fig. 9. Attention Distance of ViTs. The top two layers of EIT have less Head Diversity than LSRA. However, the deep layers (layers 3, 4, and 5) have larger Head Diversity. Overall, EIT has a larger Head Diversity. It is apparent that increasing the network’s Head Diversity improves performance. Furthermore, effective introducing IB can immediately boost deep layer Head Diversity. Compared with the other ViT and LSRA, EIT introduces IB more efficiently, resulting in better performance.

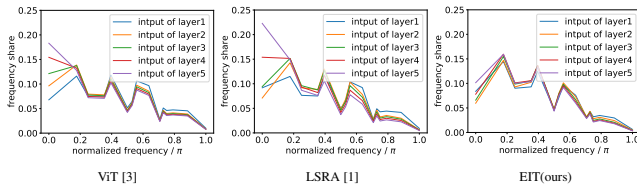


Fig. 10. Frequency Distribution of ViT, LSRA, and EIT. ViT’s HFD ($> 0\pi$) share is decreasing layer by layer, which is unfair to the deep MHAs. Compared with LFD, the deep MHAs can hardly notice HFD, which introduces to the limited attention mechanism of MHA, resulting in poor performance. Compared with ViT, the HFD share of LSRA tends to increase in the first three layers, so the MHAs can receive more HFD and shows a larger Head Diversity in Fig.9. However, the HFD share in the last two layers of LSRA is still decreasing, resulting in a small Head Diversity in Fig.9. Compared with ViT and LSRA, EIT has less reduction in HFD share per layer, ensuring an overall larger Head Diversity. It is worth noting that the Head Diversity of the EIT’s first layer is smaller than ViT and LSRA in Fig.9. We believe this is the real self-attention (the deep layers’ large Head Diversity is more important than the shallow layer) shown when each layer’s attention mechanism is improved as much as possible.

4.5. Ablation Study

On the Cifar10/100 dataset, we designed four ablation experiments based on EIT3/1/4-Mini to verify that: 1) Decreasing Structure (EIT^T) works better than Parallel Structure (Fig.3-(c)); 2) the presence or absence of convolutional layers in ELT^T is essential; 3) compared with Increasing and Invariant Structure, the Decreasing Structure is optimal; 4) EIT does not require position embedding.

4.5.1. Parallel Structure

We investigated the performance of EIT^T and Parallel Structure (Fig.3-(c)). The results are shown in Table 7. The accuracy of EIT^T is on average 2.2% higher than that of Parallel Convolution. Additionally, comparing with Parallel Convolution, EIT has only **50%** parameters and **50%** FLOPs.

Table 7. Ablations on Parallel Convolution.

TrEn with structure	FLOPs	Pram.	Cifar10	Cifar100	Avg.
	image size:32,32				
EIT ^T	0.428G	3.095M	0.855	0.605	0.730
Parallel Structure	0.887G	6.589M	0.841	0.574	0.708

4.5.2. Complicating EIT^T

We try to complicate EIT^T to see if it brings an improvement in performance. For example, we try to add multiple convolutional layers, activation layers, normalization layers, and fully connected layers. The results are shown in Table 8 showing that the one convolutional layer is the best.

Table 8. Ablations on Complicating EIT^T.

Structure of EIT ^T	FLOPs	Pram.	Cifar10	Cifar100	Avg.
	Image size:32,32				
Conv	0.428G	3.095M	0.855	0.605	0.730
None	0.527G	3.793M	0.746	0.479	0.613
Conv × 3	0.430G	3.104M	0.843	0.593	0.718
GELU, Conv, Fc	0.438G	3.170M	0.846	0.573	0.710
Conv, BN, RELU	0.429G	3.096M	0.851	0.577	0.714

4.5.3. Increasing and Invariant

We examine the performance of the Decreasing Structure of EIT^T, and the results are shown in Table 9. Compared with the Invariant Structure and Increasing Structure, the accuracy of Decreasing Structure is 9% higher on average.

4.5.4. Removing Position Embedding

Considering introducing convolutional operations in the network, we investigate whether it still requires position embedding. The results are shown in Table 10 illustrate that the impact of removing position embedding on model performance is negligible. The network without position embedding offers the possibility of simplified adaptation to more visual tasks without the need to redesign embedding.

Table 9. Ablations on Increasing and Invariant structure.

Structure	Cifar10	Cifar100	Avg.
	Image size:32,32		
Decreasing	0.855	0.605	0.730
Increasing	0.790	0.481	0.636
Invariant	0.817	0.476	0.647

Table 10. Ablations on position embedding.

Position Embedding	Cifar10	Cifar100	Avg.
	Image size:32,32		
None	0.856	0.600	0.728
Trainable	0.855	0.605	0.730

5. CONCLUSION

In this paper, we discuss why the introduction of IB improves ViT’s performance. Based on our analysis, we present a simple yet efficient network architecture that introduces IB to ViT with fewer parameters and FLOPs, called EIT. EIT ensures the efficiency of introducing IB without destroying the unification of the network in CV and NLP. Extensive experiments validate that the EIT achieves competitive performance compared with the previous representative ViTs. To the best of our knowledge, we find for the first time a strong correlation between the performance of Transformers and the diversity of head-attention distance, which gives new ideas for further improving the performance of the transformer.

6. REFERENCES

- [1] Zhanghao Wu, Zhijian Liu, Ji Lin, Yujun Lin, and Song Han, “Lite transformer with long-short range attention,” in *International Conference on Learning Representations*, 2020.
- [2] Ashish Vaswani, Noam Shazeer, Niki Parmar, Jakob Uszkoreit, Llion Jones, Aidan N. Gomez, Lukasz Kaiser, and Illia Polosukhin, “Attention is all you need,” in *Neural Information Processing Systems*, 2017, vol. 30, pp. 5998–6008.
- [3] Alexey Dosovitskiy, Lucas Beyer, Alexander Kolesnikov, Dirk Weissenborn, Xiaohua Zhai, Thomas Unterthiner, Mostafa Dehghani, Matthias Minderer, Georg Heigold, Sylvain Gelly, Jakob Uszkoreit, and Neil Houlsby, “An image is worth 16x16 words: Transformers for image recognition at scale,” in *International Conference on Learning Representations*, 2021.
- [4] Bichen Wu, Chenfeng Xu, Xiaoliang Dai, Alvin Wan, Peizhao Zhang, Masayoshi Tomizuka, Kurt Keutzer, and Peter Vajda, “Visual transformers: Token-based image representation and processing for computer vision,” *arXiv preprint arXiv:2006.03677*, 2020.
- [5] Dianxi Shi, Chenran Zhao, Yajie Wang, Huanhuan Yang, Gongju Wang, Hao Jiang, Chao Xue, Shaowu Yang, and Yongjun Zhang, “Multi actor hierarchical attention critic with rnn-based feature extraction,” *Neurocomputing*, vol. 471, pp. 79–93, 2022.
- [6] Yajie Wang, Dianxi Shi, Chao Xue, Hao Jiang, Gongju Wang, and Peng Gong, “Ahac: Actor hierarchical attention critic for multi-agent reinforcement learning,” in *2020 IEEE International Conference on Systems, Man, and Cybernetics (SMC)*, 2020, pp. 3013–3020.
- [7] Jiquan Ngiam, Aditya Khosla, Mingyu Kim, Juhan Nam, Honglak Lee, and Andrew Y Ng, “Multimodal deep learning,” in *ICML*, 2011.
- [8] Kai Han, An Xiao, Enhua Wu, Jianyuan Guo, Chunjing Xu, and Yunhe Wang, “Transformer in transformer,” in *Neural Information Processing Systems*, 2021, vol. 34.
- [9] Ze Liu, Yutong Lin, Yue Cao, Han Hu, Yixuan Wei, Zheng Zhang, Stephen Lin, and Baining Guo, “Swin transformer: Hierarchical vision transformer using shifted windows,” in *Proceedings of the IEEE/CVF International Conference on Computer Vision*, 2021, pp. 10012–10022.

- [10] Li Yuan, Yunpeng Chen, Tao Wang, Weihao Yu, Yujun Shi, Francis E. H. Tay, Jiashi Feng, and Shuicheng Yan, “Tokens-to-token vit: Training vision transformers from scratch on imagenet,” in *International Conference on Computer Vision*, 2021, pp. 558–567.
- [11] Haiping Wu, Bin Xiao, Noel Codella, Mengchen Liu, Xiyang Dai, Lu Yuan, and Lei Zhang, “Cvt: Introducing convolutions to vision transformers,” in *International Conference on Computer Vision*, 2021, pp. 22–31.
- [12] Yujing Wang, Yaming Yang, Jiangang Bai, Mingliang Zhang, Jing Bai, Jing Yu, Ce Zhang, Gao Huang, and Yunhai Tong, “Evolving attention with residual convolutions,” in *International Conference on Machine Learning*. PMLR, 2021, pp. 10971–10980.
- [13] Hugo Touvron, Matthieu Cord, Douze Matthijs, Francisco Massa, Alexandre Sablayrolles, and Herve Jegou, “Training data-efficient image transformers & distillation through attention,” in *International Conference on Machine Learning*, 2021, pp. 10347–10357.
- [14] Tete Xiao, Piotr Dollár, Mannat Singh, Eric Mintun, Trevor Darrell, and Ross Girshick, “Early convolutions help transformers see better,” *Advances in Neural Information Processing Systems*, vol. 34, 2021.
- [15] Hongyi Zhang, Moustapha Cisse, Yann N Dauphin, and David Lopez-Paz, “mixup: Beyond empirical risk minimization,” *arXiv preprint arXiv:1710.09412*, 2017.
- [16] Sangdoon Yun, Dongyoon Han, Seong Joon Oh, Sanghyuk Chun, Jun-suk Choe, and Youngjoon Yoo, “Cutmix: Regularization strategy to train strong classifiers with localizable features,” in *Proceedings of the IEEE/CVF international conference on computer vision*, 2019, pp. 6023–6032.
- [17] Zhun Zhong, Liang Zheng, Guoliang Kang, Shaozi Li, and Yi Yang, “Random erasing data augmentation,” in *Proceedings of the AAAI conference on artificial intelligence*, 2020, vol. 34, pp. 13001–13008.
- [18] Alex Krizhevsky, “Learning multiple layers of features from tiny images,” *Tech. Rep.*, 2009.
- [19] Namuk Park and Songkuk Kim, “How do vision transformers work?,” *arXiv preprint arXiv:2202.06709*, 2022.
- [20] Alex Krizhevsky, Ilya Sutskever, and Geoffrey E Hinton, “Imagenet classification with deep convolutional neural networks,” *Advances in neural information processing systems*, vol. 25, 2012.
- [21] Han Xiao, Kashif Rasul, and Roland Vollgraf, “Fashion-mnist: a novel image dataset for benchmarking machine learning algorithms,” *arXiv preprint arXiv:170807747X*, 2020.
- [22] Amirhossein Tavanaei, “Embedded encoder-decoder in convolutional networks towards explainable ai,” *arXiv preprint arXiv:200706712T*, 2020.
- [23] Ekin D Cubuk, Barret Zoph, Jonathon Shlens, and Quoc V Le, “Randaugment: Practical automated data augmentation with a reduced search space,” in *Proceedings of the IEEE/CVF Conference on Computer Vision and Pattern Recognition Workshops*, 2020, pp. 702–703.
- [24] Andrew G Howard, Menglong Zhu, Bo Chen, Dmitry Kalenichenko, Weijun Wang, Tobias Weyand, Marco Andreetto, and Hartwig Adam, “Mobilenets: Efficient convolutional neural networks for mobile vision applications,” *arXiv preprint arXiv:1704.04861*, 2017.
- [25] Kaiming He, Xiangyu Zhang, Shaoqing Ren, and Jian Sun, “Deep residual learning for image recognition,” in *Computer Vision and Pattern Recognition*, 2016, pp. 770–778.
- [26] Ilija Radosavovic, Raj Prateek Kosaraju, Ross Girshick, Kaiming He, and Piotr Dollár, “Designing network design spaces,” in *Proceedings of the IEEE/CVF conference on computer vision and pattern recognition*, 2020, pp. 10428–10436.
- [27] Zizheng Pan, Bohan Zhuang, Jing Liu, Haoyu He, and Jianfei Cai, “Scalable vision transformers with hierarchical pooling,” in *Proceedings of the IEEE/CVF International Conference on Computer Vision*, 2021, pp. 377–386.
- [28] Wenhui Wang, Enze Xie, Xiang Li, Deng-Ping Fan, Kaitao Song, Ding Liang, Tong Lu, Ping Luo, and Ling Shao, “Pvt v2: Improved baselines with pyramid vision transformer,” *Computational Visual Media*, vol. 8, no. 3, pp. 415–424, 2022.
- [29] Jiashi Li, Xin Xia, Wei Li, Huixia Li, Xing Wang, Xuefeng Xiao, Rui Wang, Min Zheng, and Xin Pan, “Next-ViT: Next Generation Vision

Transformer for Efficient Deployment in Realistic Industrial Scenarios,” *arXiv e-prints*, p. arXiv:2207.05501, July 2022.

- [30] Wenhai Wang, Enze Xie, Xiang Li, Deng-Ping Fan, Kaitao Song, Ding Liang, Tong Lu, Ping Luo, and Ling Shao, “Pyramid vision transformer: A versatile backbone for dense prediction without convolutions,” in *Proceedings of the IEEE/CVF International Conference on Computer Vision*, 2021, pp. 568–578.

A. FORMULISM EIT FOR PAPP

Formally, given a 2D image $x \in \mathbb{R}^{H \times W \times C}$, we learn a function $f(\cdot)$ that maps x_0 into new embeddings $f(x) \in \mathbb{R}^{H' \times W' \times C'}$. $f(\cdot)$ is 2D convolution operation of kernel number C' , kernel size k , stride s (in ViT, $s = k$, but in this work, $s < k$) and p padding. The height and width of the new embedding $f(x)$ take the following values.

$$H' = \lfloor \frac{H + 2p - k}{s} + 1 \rfloor, W' = \lfloor \frac{W + 2p - k}{s} + 1 \rfloor \quad (2)$$

where $\lfloor \cdot \rfloor$ denotes rounding down. The height and width of $f(x)$ then reduced by a maximum pooling (*maxpool*) layer with kernel size and stride of s_m . By adjusting s_m , we can reduce the redundant patches introduced by the convolution operation. $\text{maxpool}(f(x)) \in \mathbb{R}^{H_0 \times W_0 \times C_0}$, where $H_0 < H'$, $W_0 < W'$, $C_0 = C'$. Finally, $\mathbb{R}^{H_0 \times W_0 \times C_0}$ is transformed into $\mathbb{R}^{H_0 W_0 \times C_0}$ as the final output of EIT^P. The above descriptions can be summarized in the following expression.

$$x_0 = \text{EIT}^P(x) = \text{ReShape1D}(\text{MaxPool}(\text{Conv2D}(x))) \quad (3)$$

B. FORMULISM EIT FOR TREN

Formally, given the normalized input $x_i \in \mathbb{R}^{(1+H_i W_i) \times C_i}$ (1 represents the class embedding) of the i -layer, different channel dimensions of data are processed by MHA and EIT^T, respectively.

$$x_i^T \leftarrow \text{EIT}^T(x_i[:, : C_i^T]) \quad (4)$$

$$x_i^M \leftarrow \text{MHA}(x_i[:, -C_i^M :]) \quad (5)$$

where C_i^T and C_i^M are the number of channel dimensions processed by EIT^T and MHA, respectively, satisfying $C_i^T + C_i^M = C_i$. The $[:, :]$ is the slice operation. The final output is the combination of the output of the MHA and the EIT^T along the channel dimension.

$$x_i \leftarrow [x_i^T; x_i^M] \quad (6)$$

where the $[:, :]$ is the splicing operation of the channel dimension. The MHA is the same operation as ViT [3]. For each element in the patches $x_i \in \mathbb{R}^{(1+H_i W_i) \times C_i^M}$, we compute a weighted sum over all values v in the patches. The attention weights A_{mn} are based on the pairwise similarity between two elements of the patches and their respective query q_m and key k_n representations.

$$[q, k, v] = x_i U_{qkv}, U_{qkv} \in \mathbb{R}^{C_i^M \times C_i^{Mh}} \quad (7)$$

$$A = \text{softmax}(qk^T / \sqrt{C_i^{Mh}}), A \in \mathbb{R}^{(1+H_i W_i) \times (1+H_i W_i)} \quad (8)$$

$$HA(x_i) = Av \quad (9)$$

Multi-Head Attention (MHA) is an extension of HA in which we run k attention operations, called “heads”, in parallel, and project their concatenated outputs. To keep compute and number of parameters constant when changing k , C_i^{Mh} is typically set to C_i^M/k .

$$\begin{aligned} \text{MHA}(x_i) = \\ [HA_1(x_i[:, : C_i^{Mh}]); \dots; HA_k(x_i[:, (k-1)C_i^{Mh} :])]U_{mha}, \quad (10) \\ U_{mha} \in \mathbb{R}^{C_i^M \times C_i^M} \end{aligned}$$

Since the convolution in EIT^T handles two-dimension (2D) data, some dimensional transformations are involved before and after the convolution operation. Additionally, EIT^T does not model the class embedding because it is challenging to perform 2D convolution operations if it is added.

$$\text{EIT}^T(x_i) = [x_i'; x_i[0, :]] \quad (11)$$

$$x_i' \leftarrow \text{Reshape1D}(\text{Conv2D}(\text{Reshape2D}(x_i[1 :, :]))) \quad (12)$$

To ensure that C_i^M is divisible by h while C_i^T decreases layer by layer, for a network with a total of L -layer encoders, the C_i^T of layer i is set to

$$C_i^T = C_i - \lfloor C_i // h \times r_i \rfloor \times h \quad (13)$$

where $//$ denotes integer division, and h is the number of heads in MHA, which generally requires C_i to divide h . $r_i = i/L$, is the division ratio of C_i^T to C_i^M .

C. EFFICIENCY CONSIDERATIONS

We utilize standard convolutions in EIT^P and efficient convolutions in EIT^T. The convolutions in EIT^P are mainly for high-dimensional mapping, so the standard convolutions with high modelling capability are used. The parameters of EIT^P's convolutions are the same as ViT. Since the strides of EIT^P is smaller than the kernel size, the FLOPs of EIT^P are more than that of ViT. The redundant FLOPs are $\mathcal{O}((\frac{k^2}{s^2} - 1)3CHW)$, where C is the channel dimension and 3 is the RGB channels of images. The redundant FLOPs satisfy the linear C complexity and can be neglected compared with the C^2 complexity of TrEns. The maximum pooling in EIT^P does not require parameters, and the FLOPs are required to be $\mathcal{O}(HWC)$. It is also a linear C complexity and can be neglected compared with the C^2 complexity of TrEns.

Since the convolutions in EIT^T are mainly for increasing the locality of the same channel, the efficient convolutions are used. We split the standard $k \times k$ convolution into a depth-wise separable convolution [24] (In order not to slow down the GPU training speed, we just used one of the *depthwise* operations). Such the convolution requires $k^2 C$ parameters and $\mathcal{O}(k^2 CT)$ FLOPs, where T is the number of patches for processing. The MHA requires $4C^2 + 4C$ parameters and $\mathcal{O}(4C^2 T + T^2 C)$ FLOPs, which means that EIT^T effectively reduces the parameters and FLOPs by replacing the C^T channels of MHA with the depth-wise separable convolution.